Translational Research 280 (2025) 41–54

Contents lists available at ScienceDirect

Translational Research

journal homepage: www.elsevier.com/locate/trsl

Abundance of dopamine and its receptors in the brain and adipose tissue following diet-induced obesity or caloric restriction

Fleur W Hukema [a], Susanne Hetty [a], Christakis Kagios [a], Sofia Zelleroth [b], Giovanni Fanni [a], Maria J Pereira [a], Maria K Svensson [c,d], Magnus Sundbom [e], Anna Nilsson [b], Per E Andrén [b], Erika Roman [b,f], Jan W Eriksson [a,*]

[a] Department of Medical Sciences, Clinical Diabetology and Metabolism, Uppsala University, 751 85, Uppsala, Sweden
[b] Department of Pharmaceutical Biosciences, Uppsala University, 751 24, Uppsala, Sweden
[c] Department of Medical Sciences, Renal Medicine, Uppsala University, 751 85, Uppsala, Sweden
[d] Uppsala Clinical Research Center, Uppsala University, 751 85, Uppsala, Sweden
[e] Department of Surgical Sciences, Uppsala University, 751 85, Uppsala, Sweden
[f] Department of Animal Biosciences, Swedish University of Agricultural Sciences, 750 07, Uppsala, Sweden

ARTICLE INFO

Keywords:
Dopamine
Dopamine receptors
Obesity
Adipose tissue
Brain
Caloric restriction

ABSTRACT

While obesity and type 2 diabetes (T2D) are associated with altered dopaminergic activity in the central nervous system and in adipose tissue (AT), the directions and underlying mechanisms remain inconclusive. Therefore, we characterized changes in the abundance of dopamine, its metabolites, and receptors DRD1 and DRD2 in the brain and AT upon dietary intervention or obesity. Male Wistar rats were fed either a standard pellet diet, a cafeteria diet inducing obesity and insulin resistance, or a calorie-restricted diet for 12 weeks. Abundance of dopamine and its receptors DRD1 and DRD2 were examined in brain regions relevant for feeding behavior and energy homeostasis. Furthermore, DRD1 and DRD2 protein levels were analyzed in rat inguinal and epididymal AT and in human subcutaneous and omental AT from individuals with or without obesity. Rats with diet-induced obesity displayed higher dopamine levels, as well as DRD1 or DRD2 receptor levels in the caudate putamen and the nucleus accumbens core. Surprisingly, caloric restriction induced similar changes in DRD1 and DRD2, but not in dopamine levels, in the brain. Both diets reduced DRD1 abundance in inguinal and epididymal AT, but upregulated DRD2 levels in inguinal AT. Furthermore, in human obesity, DRD1 protein levels were elevated only in omental AT, while DRD2 was upregulated in both omental and subcutaneous AT. These findings highlight dopaminergic responses to changes in energy balance, occurring both in the brain and AT. We propose that dopaminergic pathways are involved in tissue crosstalk during the development of obesity and T2D.

Introduction

The rising prevalence of obesity has become a global health crisis, affecting nearly 1 billion individuals worldwide.[1] Obesity, and in particular excessive accumulation of fat in the visceral abdominal depot, is strongly linked with metabolic syndrome and increases the risk for type 2 diabetes (T2D) [2,3] and cardiovascular disease.[4] To support the development of effective methods to prevent and treat such disorders, it is essential to understand the underlying biological mechanisms of these diseases.

Growing evidence highlights the brain's role in the development of obesity and T2D.[5–8] Dopamine is a neurotransmitter that plays a key role in motor control, motivation, reward, cognitive function, and energy homeostasis.[9] Dopamine can bind five receptors which are categorized in two subfamilies: D1-like (DRD1 and DRD5), and D2-like (DRD2, DRD3, and DRD4),[10] and are widely expressed throughout the central

* Corresponding author. Jan W Eriksson, MD Prof, Department of Medical Sciences, Clinical Diabetology and Metabolism, Uppsala University, Akademiska sjukhuset, ingång 40, 5 t, 751 85, Uppsala, Sweden, Tel: +46 186114419.

E-mail addresses: fleur.hukema@uu.se (F.W. Hukema), susanne.hetty@medsci.uu.se (S. Hetty), christakis.kagios@medsci.uu.se (C. Kagios), sofia.zelleroth@uu.se (S. Zelleroth), giovanni.fanni@medsci.uu.se (G. Fanni), maria.pereira@medsci.uu.se (M.J. Pereira), maria.k.svensson@ucr.uu.se (M.K. Svensson), magnus.sundbom@uu.se (M. Sundbom), anna.m.nilsson@uu.se (A. Nilsson), per.andren@uu.se (P.E. Andrén), erika.roman@slu.se (E. Roman), jan.eriksson@medsci.uu.se (J.W. Eriksson).

https://doi.org/10.1016/j.trsl.2025.05.001
Received 14 March 2025; Received in revised form 5 May 2025; Accepted 5 May 2025
Available online 8 May 2025

nervous system (CNS). In the past decades, obesity has been associated with changes in dopamine signaling in the CNS, leading to detrimental effects on energy and glucose homeostasis.[11–13] However, both decreased and increased availability of striatal DRD2 have been linked to human obesity.[13–15] Furthermore, altered dopamine receptor expression patterns were found in the nucleus accumbens (NAc) in animal models of obesity.[16] Interestingly, the DRD2 agonist bromocriptine, a medication used for Parkinson's disease and hyperprolactinemia, was found to improve glucose homeostasis via its dopamine-mimicking and subsequent sympatholytic effects and is currently approved for the treatment of T2D in the US.[17,18] Furthermore, central DRD2 stimulation with bromocriptine in the lateral hypothalamus (LH) was shown to increase adipose tissue (AT) activity, and decrease body weight (BW) gain and white AT mass in rodents.[19] This indicates that changes in central dopamine signaling are relevant for peripherally elicited metabolic effects.

The brain communicates with AT partly via sympathetic nerves expressing tyrosine hydroxylase (TH) that innervate the AT to regulate processes such as lipolysis, adipogenesis, and thermogenesis.[20] TH catalyzes the first and rate-limiting step in the synthesis of dopamine [21] and is used as a sympathetic innervation and activity marker in AT.[22–24] Dopamine can be released via exocytosis from sympathetic nerves to bind to dopamine receptors in AT.[25] Our group has previously shown DRD1 and DRD2 in subcutaneous AT (SAT) to be implicated in lipid and glucose metabolism in humans.[26] Furthermore, both obesity and T2D alter the expression of DRD1, DRD2, and TH in AT in rodents and humans.[22,26–28] Nevertheless, there is limited knowledge from animal models and human data on the regulation of dopaminergic signaling in AT in metabolic disorders.

In the present study, we used a diet-induced obesity (DIO) model in adult rats that effectively induced obesity and mild-moderate metabolic impairments, in particular an insulin-resistant prediabetic state. The metabolic and behavioral characteristics of this model were recently published.[29] Herein, we primarily aimed to study the impact of obesity on the abundance of DRD1 and DRD2, as well as the abundance and metabolism of dopamine in key brain regions involved in reward, motivation, and regulation of energy and glucose metabolism. These regions included the cingulate cortex (Cg), caudate putamen (CPu), NAc core and shell, anterior hypothalamus (AH), ventromedial hypothalamus (VMH), and the LH. These regions are involved in the three major dopaminergic systems in the brain. The mesocorticolimbic pathway arises from the ventral tegmental area (VTA) and projects to both limbic and cortical regions. Mesocortical neurons project to the prefrontal cortex, including the Cg, regulating executive functions, while the mesolimbic neurons project to the NAc and the olfactory tubercle to regulate reward processing and motivation.[30] The CPu is part of the nigrostriatal pathway and receives input from the substantia nigra to regulate motor control and habit formation, but is also implicated in reward processing.[31] Lastly, the tuberoinfundibular pathway connects the hypothalamus to the pituitary gland, where dopamine is involved in hormone secretion [32] and energy homeostasis.[33]

In parallel, we addressed changes in DRD1, DRD2, and TH in inguinal (iWAT) and epididymal white adipose tissue (eWAT), respectively corresponding to SAT and visceral AT. Additionally, we analyzed these parameters under the converse condition, aiming at counteracting weight gain by analyzing rats subjected to caloric restriction (CR). Finally, we explored the DIO model in relation to human obesity. Hence, we assessed DRD1, DRD2, and TH protein levels in human SAT, and omental AT (OAT), representing the visceral abdominal depot, from individuals with or without obesity but without T2D. To the best of our knowledge, this is the first study exploring effects of obesity on dopamine metabolism and dopamine receptors simultaneously in key brain areas involved in feeding behavior and energy balance. Likewise, there are no studies investigating DRD1, DRD2, and TH protein levels in human OAT from individuals with or without obesity.

Methods

Animals and diets

The animal experiments were approved by the Uppsala Animal Ethical Committee (permit number 5.8.18-12996/2022) and followed the guidelines of the Swedish Legislation on Animal Experimentation (Animal Welfare Act SFS 2018:1192) and the European Union Directive on the Protection of Animals Used for Scientific Purposes (Directive 2010/63/EU). The animal work is reported in accordance with the ARRIVE reporting guidelines.[34]

The experimental design and metabolic characteristics of the animals have been described previously.[29] Briefly, 36 8-week-old male Wistar rats (RccHan:WI, Envigo, Horst, the Netherlands) were pair-housed in transparent type IV cages under a reversed 12-h light/dark cycle, controlled temperature (22 ± 1°C) and humidity (50 ± 10%). Upon arrival, the rats were left undisturbed for two weeks for acclimatization and adaptation to the reversed light/dark cycle. The rats were thereafter randomized into three groups of n=12; a control group with ad libitum access to standard chow (ssniff Spezialdiäten GmbH, Germany), a DIO group fed simultaneous ad libitum standard chow, chocolate balls, cheese doodles, and roasted, salted peanuts spread throughout the cage; and a CR group receiving an amount of standard chow adjusted to maintain the rats at 85% of the BW of the control group.[29] After 12 weeks of diet, all animals were briefly anesthetized and euthanized by decapitation for the collection of the brain, iWAT, and eWAT. Brains were frozen in -20°C isopentane, and AT samples in liquid nitrogen, and then stored in -80°C until further analyses.[29]

Dopamine and its metabolites, as well as DRD1 and DRD2 receptor levels, were analyzed in the selected brain regions from 18 rats that were chosen from the cohort based on BW.[29] To ensure a clear distinction of phenotypes between groups, the six rats with the highest BW in the DIO group and the six rats with the lowest BW in the CR group were selected. The six rats with a BW closest to average were selected in the control group. DRD1, DRD2, and TH protein levels were assessed in AT from 32 rats (8 control, 12 DIO, and 12 CR). TH protein levels were used as a sympathetic innervation marker. The metabolic parameters of the rats included in the brain and AT analyses are presented in Supplementary Table 1. Not all assessments could be performed in all rats and the n/group is specified in the figure or table legends.

Human adipose tissue donors

The study was approved by the Regional Ethics Review Board in Uppsala (Dnr 336-07, T 508-09, Dnr 2020-06350, Dnr 2013-183/494, and Dnr 2018/385) and conducted in accordance with the principles of the Declaration of Helsinki. All participants provided written informed consent.

All subjects were recruited at the Uppsala University Hospital. Paired SAT and OAT samples were collected from 8 lean subjects (BMI < 25.0 kg/m^2, 3F/5M) and 8 subjects with obesity (BMI > 30.0 kg/m^2, 5F/3M), all without diabetes, undergoing kidney donation [35] or obesity surgery,[26] respectively, at Uppsala University Hospital. Exclusion criteria were endocrine disorders, cancer, or other major illnesses, and ongoing medication with beta-adrenergic blockers, systemic glucocorticoids, modulators of dopamine signaling, or immune-modulating therapies. Baseline clinical evaluation included a complete medical history and clinical examination. The patients' anthropometric measurements, and hematological and biochemical parameters are described in Supplementary Table 2. Anthropometrics were assessed and blood samples were taken after an overnight fast (>10h) for measurements of HbA1c, glucose, and insulin levels. AT samples were snap-frozen in liquid nitrogen and used for protein expression analysis according to a previously reported protocol,[26] with slight modifications.

Rat brain preparation

Frozen brains were equilibrated for 30 min at -20°C in a cryo-chamber. Using a cryostat-microtome (Leica CM3050 S, Leica Microsystems, Germany), 12 μm coronal sections were cut at +2.28 mm and -2.16 mm from Bregma.[36] The researcher sectioning the brains was unaware of the treatment groups. For matrix-assisted laser desorption/ionization mass spectrometry imaging (MALDI-MSI) analysis, brain sections from rats in each treatment group were thaw-mounted next to each other on pre-cooled indium tin oxide-coated (ITO) glass slides (Bruker Daltonics, Germany) to minimize variation due to matrix application and MSI data acquisition. For immunohistochemistry, consecutive brain sections from each sample were thaw-mounted on Superfrost™ Plus adhesion microscope slides (Epredia, Netherlands). Samples were kept at -80°C until further analysis.

MALDI-MSI

Dopamine is degraded via two primary metabolic routes into homovanillic acid (HVA, Fig. 1G). Dopamine that is leaked from presynaptic vesicles or that is taken up via the dopamine reuptake transporter after release is converted by monoamine oxidase (MAO) to 3,4-dihydroxyphenylacetaldehyde (DOPAL), which is metabolized to 3,4-dihydroxyphenylacetic acid (DOPAC) and finally to HVA.[37] After release, dopamine in the synaptic cleft is metabolized to 3-MT by the action of catechol-O-methyltransferase (COMT), and converted to HVA.[38] In this project, the HVA content and HVA/dopamine ratio in the different brain regions are used as a proxy of overall dopamine turnover.[38]

MALDI-MSI was used to image dopamine, the first metabolites in the two metabolic routes DOPAL and 3-MT, and the end-product HVA in accordance with a previously described protocol,[39,40] with minor modifications. ITO-slides were put in a vacuum desiccator for 30 min. The reactive MALDI derivatization matrix 4-(anthracene-9-yl)-2--fluoro-1-methylpyridin-1-ium iodide salt (FMP-10; Tag-ON AB, Uppsala, Sweden) was dissolved in 70% acetonitrile (Merck, Darmstadt, Germany) to a concentration of 1.8 mg/ml, briefly sonicated and sprayed over the tissue sections using a robotic sprayer (TM-Sprayer, HTX-Technologies, USA). Parameters of the spraying method were: temperature, 80°C; nitrogen gas pressure, 6 psi; pump flow rate, 80 ml/min; nozzle velocity, 1100 mm/min; number of passes, 20; track spacing, 2mm track. Slides were optically imaged using a flatbed photo scanner (Epson Perfection V500, Japan). MSI experiments were carried out on a solariX 7T-2ω MALDI-Fourier-transform ion cyclotron resonance MS instrument (Bruker Daltonics), equipped with a SmartBeam II 2 kHz Nd:YAG laser, operated in positive ion mode with quadrature phase detection. Data was collected across the mass-to-charge (m/z) range of 150-1500, with the time-of-flight value at 0.7 ms, and frequency at 4MHz. The method was calibrated with red phosphorus and online calibration was performed using the FMP-10 ion cluster (m/z 555.2231) as lock mass and the quadrupole isolation m/z ratio was set at m/z 379 deflecting the high abundant FMP-10 peak. Molecular images were acquired at a lateral resolution of 120 μm. Sections were analyzed in random order to prevent possible bias due to variation in mass spectrometer sensitivity. Data was visualized using FlexImaging (v.5.0, Bruker Daltonics) and further analysed in SCiLS Lab (v.11, Bruker Daltonics) in which the Cg, CPu, NAc core and shell, and the hypothalamus (Hth) were annotated according to the Rat Brain in Stereotaxic Coordinates Atlas.[36] Dopamine, 3MT, DOPAL, and HVA were identified according to the accurate m/z value (Supplementary Table 3), the anatomical brain distribution, and previously acquired tandem MS data from rat brain tissue.[39,40] Root-mean-square (RMS) normalized average ion intensity values of the peak area were exported from SCiLS Lab for all analytes in the areas of interest.

Rat brain immunohistochemistry

Fresh frozen cryo-tissue sections were air-dried at room temperature (RT), and fixed with ice-cold 100% methanol for 10 min at -20°C. Sections were washed three times in 1x Phosphate-buffered saline (PBS) and then incubated with Blocking buffer: 5% normal goat serum and 0.3% Triton X-100 (Sigma, T-8787) in 1x PBS for one hour at RT. Then, sections were incubated for 72 hours at 4°C with primary antibody anti-DRD1 (1:100, Sigma, D2944, RRID:AB_1840787), anti-DRD2 (1:50, Merck, Ab5084P, RRID:AB_2094980), or TH (1:100, Sigma, ZMS1033), dissolved in Blocking buffer. After incubation, sections were washed in 1x PBS and incubated with secondary Goat-anti-Rabbit Alexa Fluor-488 (1:200, Invitrogen, 2521157), Goat-anti-Rat Alexa Fluor-647 (1:200, Invitrogen, A48265), or Goat-anti-Mouse Alexa Fluor-647 (1:1000, Invitrogen, A21236) for two hours at RT. After final washing with 1x PBS, sections were mounted with SlowFade Diamond Antifade Mountant with DAPI (Invitrogen, S36968). Brain slices were imaged on the ImageXpress® Pico Automated Cell Imaging System (Molecular Devices), using a 10x objective. Qupath (v0.5.1) was used to annotate the Cg, CPu, NAc Core and Shell, AH, VMH and LH according to the Rat Brain in Stereotaxic Coordinates Atlas.[36] Images were exported to Image J, FIJI (v.2.14.0/1.54f) to measure the mean fluorescence intensity (mfi), which was corrected for background intensity.

Adipose tissue immunoblotting

Detailed immunoblotting methods are described in the Supplementary Methods. Briefly, rat and human AT were homogenized with lysis buffer. The infranatant was collected, and protein concentration was determined. 15 μg protein lysates were separated by SDS-PAGE and transferred to membranes. Stain-free blot imaging was used to quantify the total protein of each sample and to normalize the target protein levels. Membranes were incubated overnight at 4°C with primary antibody anti-DRD1 (1:1000, Sigma, D2944), anti-DRD2 (1:1000, Merck, Ab5084P), or TH (1:1000, Sigma, ZMS1033), followed by incubating with horse-radish peroxidase-conjugated goat-anti-rat (1:2000, Cell Signaling, 7077), goat-anti-rabbit (1:2000, Cell Signaling, 7074), or goat-anti-mouse (1:2000, Cell Signaling, 7076) for one hour. Protein bands and stain-free blots were imaged using a ChemiDoc™ MP Imaging System (Bio-Rad, 12003154). Proteins were quantified using Image Lab Software (Bio-Rad, v6.1.0).

Statistics

Data are presented as mean ± SEM, unless stated otherwise. Normality of data was first assessed using the Shapiro-Wilk W test, and normal distribution of the residuals was evaluated through visual validation of Q–Q plots. Non-normally distributed data were log-transformed before analysis and back-transformed to the original scale for presentation. Comparisons between two groups were made using unpaired t-tests. A one-way ANOVA was used to assess differences among three groups and post-hoc comparisons were only conducted between the DIO or CR versus the control group using the false discovery rate Benjamini, Krieger, and Yekutieli method. Human AT data were analyzed using a mixed-model ANOVA and the false discovery rate (Benjamini, Krieger, and Yekutieli) was used for multiple comparisons correction. Spearman's correlation was used to test for bivariate analyses, and significant variables were included in a multilinear regression model to predict their impact on dopamine levels in the NAc core, or DRD1 and TH protein levels in iWAT. Sample sizes were determined based on previous studies investigating the effects of dietary interventions in rats.[41,42] For this exploratory research focusing on dopamine and its receptors, no formal power analysis was performed. However, a post-hoc calculation indicated that the study had 80% power to detect a 25% difference in brain dopamine abundance between groups (n=6/group, α=0.05). P-values below 0.05 were considered

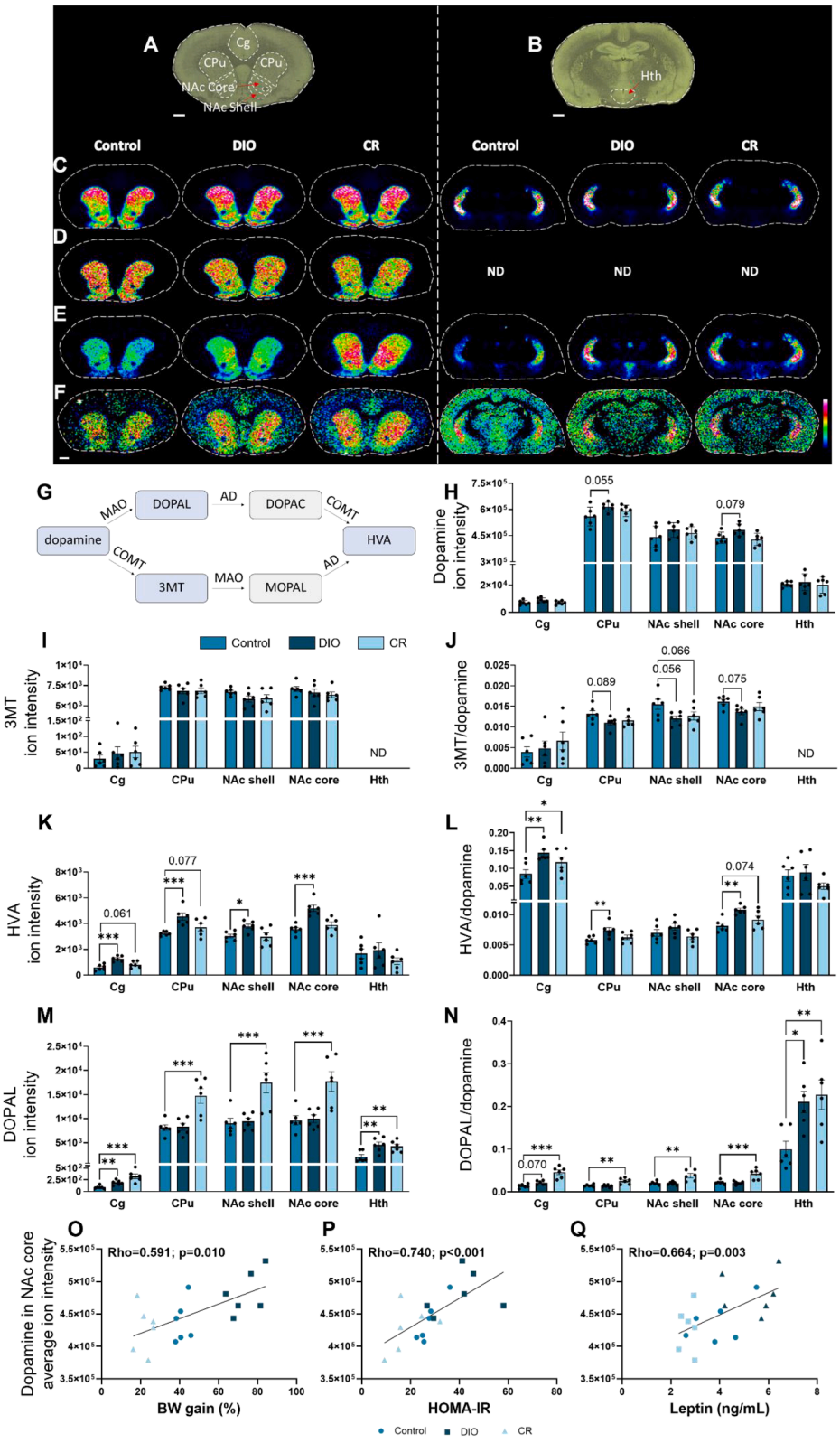

(caption on next page)

Fig. 1. Dopamine, dopamine metabolites, and dopamine receptors DRD1 and DRD2 in brains from control, DIO, and calorie-restricted rats. Imaging experiments were conducted on brain tissue sections from control rats, rats with diet-induced obesity (DIO), or calorie-restricted (CR) rats (n=6/group). Optical images of coronal brain tissue at Bregma +2.28 mm (A), showing the cingulate cortex (Cg), caudate putamen (CPu), nucleus accumbens core (NAc core) and shell (NAc shell, left panel), or Bregma -2.16 mm (B), showing the hypothalamus (Hth, right panel). The MALDI-MSI images show the distribution of metabolites from the dopaminergic metabolic pathway: dopamine (C), 3-methoxytyramine (3MT, D), 3,4-dihydroxyphenylacetaldehyde (DOPAL, E), and homovanillic acid (HVA, F). Color scaling from ion intensity from 0 to 100%. Data are normalized against the root mean square. Scale bar is 1 mm. Overview of the dopaminergic metabolic pathway (G); dopamine, 3MT, DOPAL and HVA were analyzed and highlighted in blue. Regional quantification of dopamine (H), 3MT (I), 3MT/dopamine ratio (J), HVA (K), HVA/dopamine ratio (L), DOPAL (M), DOPAL/dopamine ratio (N) in the Cg, CPu, NAc shell and core, and the Hth. Data are shown as individual rats and mean ± SEM. Spearman's Rho correlations across all groups (n=6/group) between dopamine levels in the NAc core and BW gain (O), HOMA-IR (P), and leptin levels (Q) in individual control (●), DIO (■), or CR (▲) rats. * p<0.05, ** p<0.01, *** p<0.001. Abbreviations: AD, aldehyde dehydrogenase; BW, body weight; COMT, Catechol-O-Methyltransferase; DOPAC, 3,4-dihydroxyphenylacetic acid; MAO, monoamine oxidase; MOPAL, 3-methoxy-4-hydroxyphenylacetaldehyde; ND, not detected.

statistically significant. All data were analyzed using GraphPad Prism 10.4.1 or IBM SPSS version 28.0.1.0.

Results

Adiposity measures

The metabolic parameters of the rats included in the brain and AT analyses, a subset of the original cohort,[29] are displayed in Supplementary Table 1. After 12 weeks of diet, the DIO rats displayed significantly higher BW compared to controls (576 ± 43 g vs 493 ± 27 g, p<0.001), while CR rats had significantly lower BW compared to controls (424 ± 21 g, p<0.001). Homeostatic Model Assessment for Insulin Resistance (HOMA-IR) index was significantly higher in DIO rats compared to controls (36.9 ± 9.5 vs 25.7 ± 7.9, p<0.01), thus reflecting a prediabetic state. Relative eWAT weight was also significantly increased in DIO rats compared to controls (41.0 ± 7.2 vs 16.9 ± 5.7, p<0.001), but not different between CR and control rats (Supplementary Table 1).

Dopamine and its metabolites in brain regions involved in reward, motivation, and energy homeostasis following diet-induced obesity or caloric restriction

Dopamine, 3MT, HVA, and DOPAL were simultaneously visualized in the Cg, CPu, NAc shell and core, and the Hth (Fig. 1A-1F). The dopamine degradation pathway with enzymes is depicted in Fig. 1G. DIO, but not CR, tended to increase dopamine levels in the CPu (p=0.055 vs control), and the NAc core (p=0.079 vs control), while neither diet changed dopamine abundance in the Cg, NAc shell, or Hth (Fig. 1H). 3MT levels were unchanged by both dietary interventions in the Cg, CPu, NAc shell and core, and were below the detection limit in the Hth (Fig. 1I). DIO tended to decrease the 3MT/dopamine ratio in the CPu (p=0.089), NAc shell (p=0.056), and the NAc core (p=0.075), compared to control. In the NAc shell, a similar trend was observed following CR (p=0.066 vs control, Fig. 1J). DIO increased HVA levels in the Cg (p<0.001), CPu (p<0.001), NAc shell (p<0.05) and NAc core (p<0.001), compared to control (Fig. 1K). CR tended to increase HVA levels in the Cg (p=0.061 vs control), and the CPu (p=0.077 vs control, Fig. 1K). DIO increased the HVA/dopamine ratio in the Cg, CPu, and NAc core, compared to control (p<0.01 for all). CR increased the HVA/dopamine ratio in the Cg (p<0.05 vs control) and tended to increase in the NAc core as well (p=0.074 vs control, Fig. 1L). CR increased DOPAL levels in all brain regions analyzed in this study (p<0.001 vs control for the Cg, CPu, NAc shell and NAc core, p<0.01 for the Hth, Fig. 1M). CR also increased the DOPAL/dopamine ratio in all brain regions analyzed in this study (p<0.001 vs control for the Cg and NAc core, p<0.01 for the CPu, NAc shell and Hth, Fig. 1N). DIO increased DOPAL levels in the Cg and Hth, compared to control (p<0.01 for both, Fig. 1M). The DOPAL/dopamine ratio was increased by DIO in the Cg, although not statistically significant (p=0.070 vs control), and in the Hth (p<0.05 vs control, Fig. 1N).

Across all groups, dopamine abundance in the NAc core positively correlated with BW (p<0.05), BW gain (p<0.01, Fig. 1O), relative eWAT weight (p<0.05), and leptin (p<0.01, Fig. 1Q), as well as HOMA-IR (p<0.001, Fig. 1P), insulin and adiponectin levels (p<0.01 for both, Supplementary Table 4). Multiple regression analysis (adjusted R^2=0.398) revealed HOMA-IR (β=0.592, p=0.054) as a stronger predictor of dopamine levels in the NAc core than BW (β=0.118, p=0.684). In a model that included both HOMA-IR and BW gain (adjusted R^2=0.440), neither variable reached significance (β=0.460, p=0.103 for HOMA-IR, and β=0.302, p=0.273 for BW gain). Dopamine levels in the Cg correlated positively with relative eWAT weight and adiponectin levels (p<0.05 for both). Dopamine levels in the CPu were associated with relative eWAT weight and HOMA-IR (p<0.05 for both, Supplementary Table 4).

DRD1 and DRD2 abundance in brain regions involved in reward, motivation, and energy homeostasis following diet-induced obesity or caloric restriction

We next examined the effects of DIO or CR on DRD1 and DRD2 protein levels in the Cg (Fig. 2A), CPu, NAc core and shell (Fig. 2B), AH, VMH, and LH (Fig. 3A). Both DIO and CR increased DRD1 protein levels in the Cg (p<0.05 vs control for both, Fig. 2C), while DRD2 levels remained unchanged by both diets (Fig. 2D). Both DRD1 and DRD2 protein levels in the CPu were increased following DIO (p<0.05 for both, Fig. 2E and 2F). DRD1 and DRD2 protein levels in the CPu were also increased following CR (p<0.01 for DRD1, p<0.05 for DRD2, Fig. 2E and 2F). Neither diet changed DRD1 protein levels in the NAc core (Fig. 2G), NAc shell (Fig. 2I), AH (Fig. 3B), VMH (Fig. 3D), and LH (Fig. 3F). Both diets tended to increase DRD2 protein levels in the NAc Core (p=0.091 for both, Fig. 2H), while neither diet changed DRD2 protein levels in the NAc shell (Fig. 2J). DRD2 protein levels remained unchanged by both diets in the AH (Fig. 3C). DIO increased DRD2 protein levels in the VMH, compared to control (p<0.05, Fig. 3E), and tended to increase in the LH as well (p=0.087 vs control, Fig. 3G).

Multiple linear regression analyses including a quadratic term revealed a significant U-shaped relationship between BW and DRD2 protein levels in the Cg and CPu (p<0.01 for both, Supplementary Figure 1C and D, respectively). Similar results were found between BW and DRD2 in the NAc Core (data not shown). A U-shaped pattern was also observed between BW and DRD1 protein levels in the CPu (p<0.05) but not in the Cg (Supplementary Figure 1A and B, respectively).

DRD1, DRD2, and TH protein levels in rat inguinal and epididymal adipose tissue

In iWAT, DRD1 protein levels were ~50% lower following DIO (p<0.001) and 41% lower following CR (p<0.01), compared to control (Fig. 4A). DIO increased DRD2 protein in iWAT by 56% (p<0.05 vs control), while CR increased DRD2 protein levels by 38% (p<0.05 vs control, Fig. 4B). DIO reduced TH in iWAT by 61% (p<0.001 vs control), while CR had no effect (Fig. 4C). Both diets decreased DRD1 in eWAT by ~41% (p<0.01 vs control for both, Fig. 4D), while DRD2 and TH levels in eWAT remained unchanged (Fig. 4E and 4F, respectively).

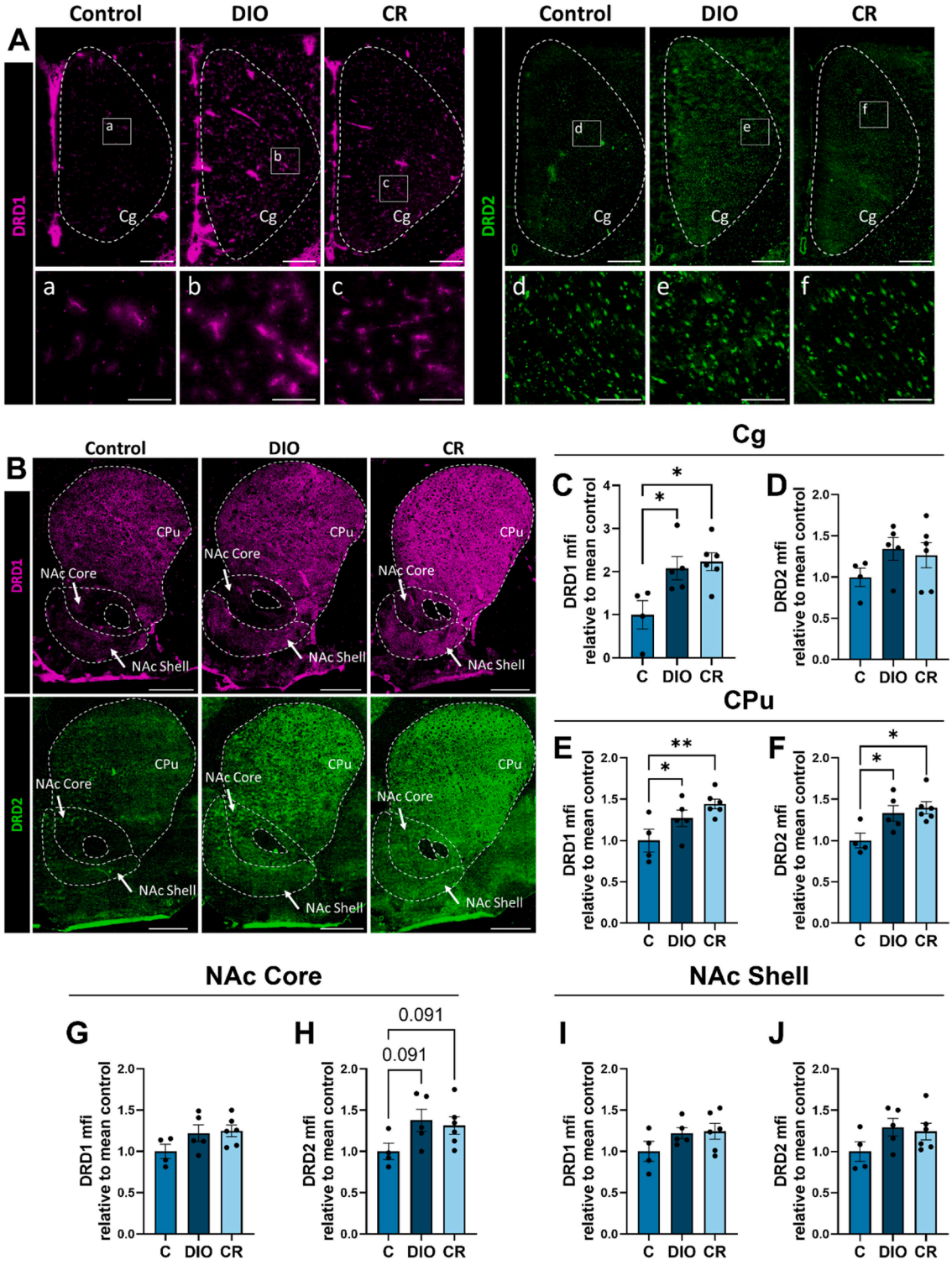

Fig. 2. DRD1 and DRD2 abundance in brains from control, DIO, and calorie-restricted rats. Immunofluorescence staining of DRD1 (purple) and DRD2 (green) of coronal brain sections (Bregma +2.28 mm), showing the Cg (A), and CPu and the NAc core and NAc shell (B) in control, DIO, or CR rats. Quantification of DRD1 and DRD2 in the Cg (C and D), CPu (E and F), NAc core (G and H), NAc shell (I and J). 10x magnification. Data are shown as individual rats and mean ± SEM (n=4-6/group). Values are relative to the mean of the control group. * $p<0.05$, ** $p<0.01$. In A, the scale bar is 500 μm, and 200 μm for the zoomed images. Scale bar for B is 1 mm. Abbreviations: C, control; Cg, cingulate cortex; CPu, caudate putamen; CR, caloric restriction; DIO, diet-induced obesity; mfi, mean fluorescence intensity; NAc, nucleus accumbens.

We then assessed the relationship between DRD1, DRD2, and TH protein levels in iWAT and eWAT with markers of adiposity, hyperglycemia and insulin resistance after 12 weeks of dietary intervention within groups (Table 1) and across all groups (Fig. 4G-I and Supplementary Table 5). In the control group, DRD1 protein levels in iWAT negatively correlated with glucose levels ($p=0.05$). In the DIO group, DRD1 in iWAT showed the same negative direction but did not reach significance ($p=0.110$, Table 1). In the CR group, DRD2 protein

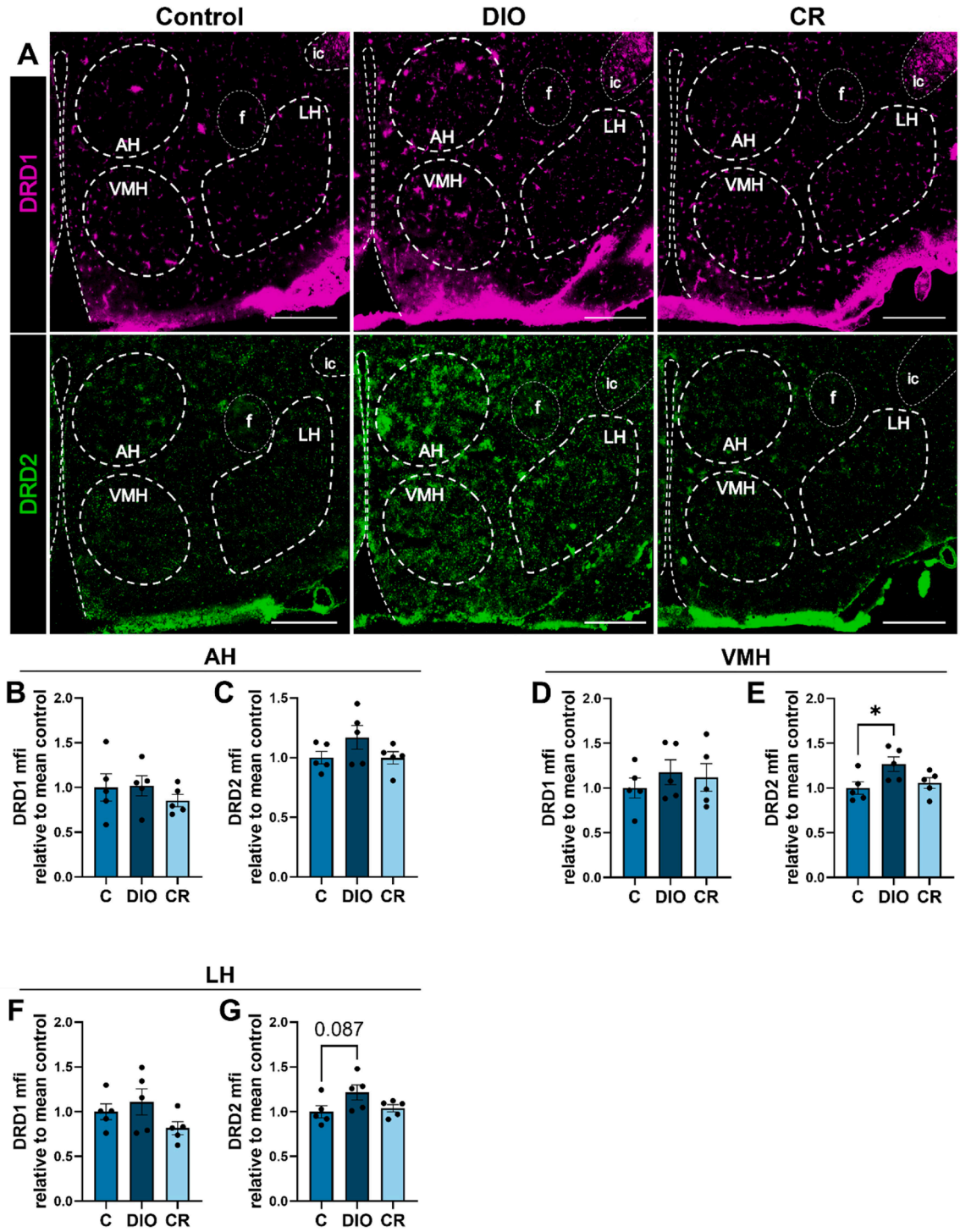

Fig. 3. DRD1 and DRD2 abundance in hypothalamic areas of control, DIO, and calorie-restricted rats. Immunofluorescence staining of DRD1 (purple) and DRD2 (green) of coronal brain slices (Bregma –2.16 mm), showing the anterior hypothalamus (AH), ventromedial hypothalamus (VMH) and lateral hypothalamus (LH) in control, DIO, or CR rats (A). Quantification of DRD1 and DRD2 in the AH (B and C), and VMH (D and E), and the LH (F and G). 10x magnification. Data are shown as individual rats and mean ± SEM (n=5/group). Values are relative to the mean of the control group. * $p<0.05$. Scale bar is 500 μm. Abbreviations: C, control; CR, caloric restriction; DIO, diet-induced obesity; f, fornix; ic, internal capsule; mfi, mean fluorescence intensity.

levels in iWAT correlated positively with BW gain ($p<0.01$) and leptin levels ($p<0.05$, Table 1). In the control group, TH protein levels were negatively correlated with HOMA-IR and insulin levels ($p<0.05$ for both, Table 1).

Across all groups, DRD1 protein levels in iWAT negatively correlated with relative eWAT weight, glucose, and adiponectin levels ($p<0.05$ for all), whereas DRD2 was not associated with the markers analyzed (Supplementary Table 5). TH protein levels in iWAT negatively correlated with BW gain ($p<0.001$, Fig. 4G), HOMA-IR ($p=0.001$, Fig. 4H) and leptin levels ($p<0.01$, Fig. 4I), and also with BW and eWAT weight ($p<0.001$ for both), insulin ($p<0.05$), glucose ($p<0.01$), and adiponectin levels ($p<0.001$, Supplementary Table 5). We determined the strongest predictors of DRD1 and TH protein levels in iWAT with multilinear regression models (Table 2). For both proteins, the model

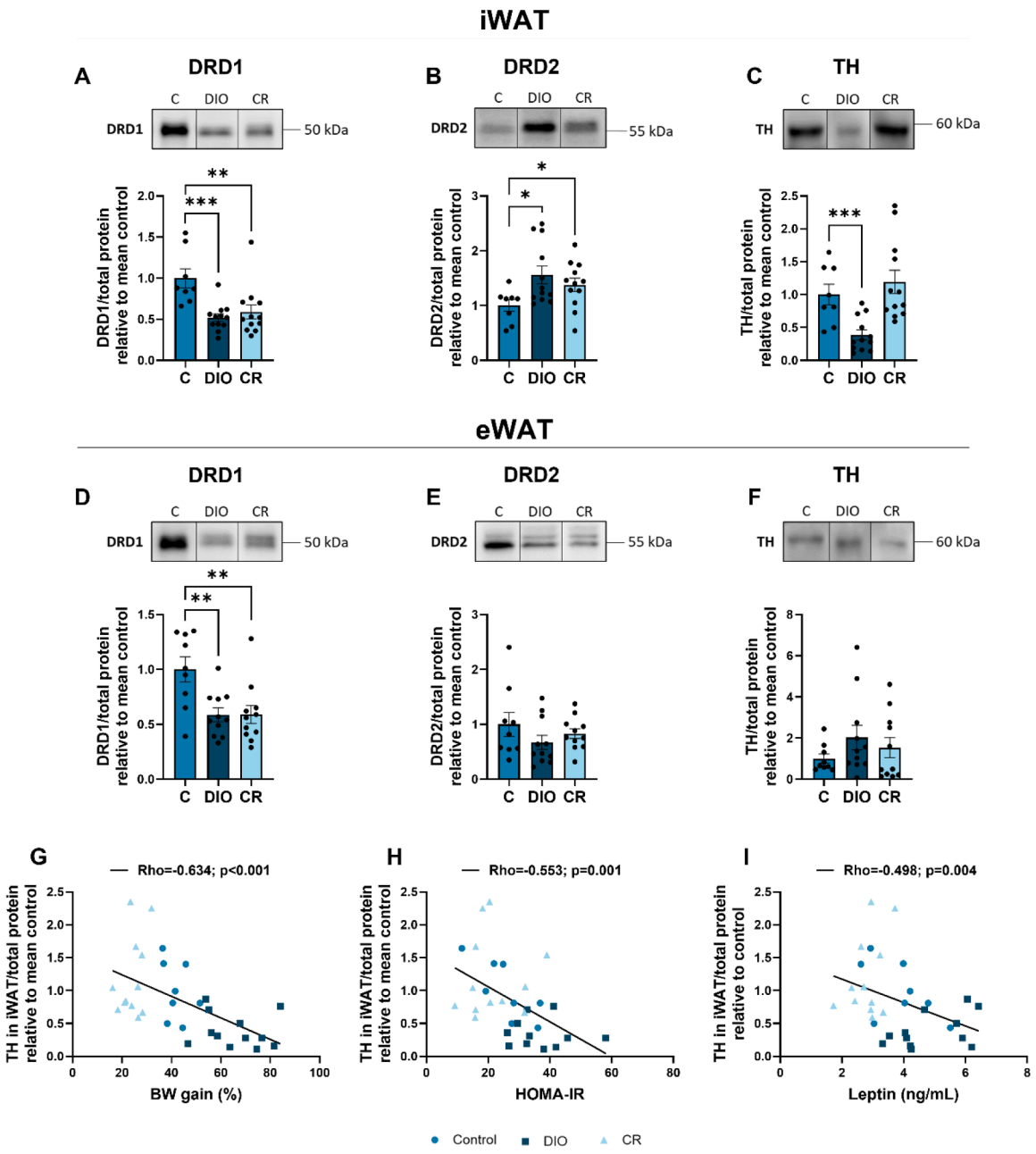

Fig. 4. DRD1, DRD2 and TH protein levels in rat iWAT and eWAT, and correlations between TH in iWAT and BW gain, HOMA-IR and leptin levels. Representative immunoblot and protein quantification of DRD1, DRD2, and TH protein levels in iWAT (A-C) and eWAT (D-F) from control, DIO, or calorie-restricted (CR) rats. Representative bands are derived from three parts of the same gel. Protein levels were normalized to total protein (Supplementary Figure 2) and to a reference sample loaded on each gel. Values are relative to the mean of the control group. Data are shown as mean ± SEM (n=8-12/group). Spearman's Rho correlations between TH protein levels in iWAT and BW gain (G), HOMA-IR (H), and leptin levels (ng/mL, I) in individual control (●), DIO (■), or CR (▲) rats. * $p<0.05$, ** $p<0.01$, *** $p<0.001$. Abbreviations: C, control; BW, body weight; CR, caloric restriction; DIO, diet-induced obesity; eWAT, epididymal white adipose tissue; iWAT, inguinal white adipose tissue; TH, tyrosine hydroxylase.

included group (diet), BW gain, and glucose levels. Despite the absence of a linear correlation between DRD1 protein levels in iWAT and BW gain (Supplementary Table 5), multilinear regression revealed BW gain as a significant independent predictor ($p<0.01$) after adjusting for group (diet) and glucose levels (Table 2). Group (diet) and glucose levels were also significant predictors of DRD1 protein levels in iWAT ($p<0.001$ and $p<0.05$, respectively). For TH protein levels in iWAT, group (diet) was not significant, while BW gain and glucose levels were both significant predictors ($p<0.01$ and $p<0.05$, respectively, Table 2). Alternative models, including BW or HOMA-IR, were weaker in predicting DRD1 or TH protein levels in iWAT (data not shown).

In the control group, DRD1 protein levels in eWAT tended to correlate positively with relative eWAT weight ($p=0.077$). This correlation was negative within the DIO group but did not reach statistical significance ($p=0.110$, Table 3). In the CR group, DRD1 protein levels in eWAT correlated negatively with BW gain ($p<0.01$). In the control group, DRD2 protein levels in eWAT correlated negatively with BW and leptin levels ($p<0.01$ and $p<0.05$, respectively), and tended to correlate negatively with relative eWAT weight ($p=0.058$), HOMA-IR ($p=0.077$), and insulin levels ($p=0.099$) as well (Table 3). In the CR group, the correlations between DRD2 protein levels in eWAT and BW and leptin were positive ($p<0.05$ for BW, $p<0.01$ for leptin, Table 3). In the control

Table 1
Correlations of DRD1, DRD2, and TH protein levels in rat iWAT with markers of obesity, hyperglycemia and insulin resistance within the control, DIO, or restricted group.

iWAT	DRD1						DRD2						TH					
	Control		DIO		CR		Control		DIO		CR		Control		DIO		CR	
	Rho	p-value	Rho	p-value	Rho	p-value	Rho	p-value	Rho	p-value	Rho	p-value	Rho	p-value	Rho	p-value	Rho	p-value
Adiposity measures																		
BW (g)	0.286	0.493	-0.469	0.124	0.224	0.484	0.571	0.139	-0.056	0.863	0.371	0.236	-0.333	0.420	-0.224	0.484	0.462	0.131
BW gain (%)	-0.190	0.651	-0.217	0.499	0.112	0.729	0.095	0.823	0.406	0.191	**0.783**	**0.003**	-0.500	0.207	-0.245	0.443	0.112	0.729
eWAT (g/kg)	-0.238	0.570	*-0.524*	*0.080*	0.084	0.795	0.095	0.823	0.042	0.897	-0.056	0.863	*-0.643*	*0.086*	0.070	0.829	-0.294	0.354
Leptin	0.119	0.779	-0.189	0.557	-0.112	0.729	0.071	0.867	0.406	0.191	**0.601**	**0.039**	*-0.643*	*0.086*	0.322	0.308	0.028	0.931
Hyperglycemia and insulin resistance																		
HOMA-IR[a]	-0.595	0.120	-0.209	0.537	-0.070	0.829	-0.095	0.823	-0.082	0.811	0.217	0.499	**-0.810**	**0.015**	-0.164	0.631	0.252	0.430
Plasma insulin	-0.333	0.420	-0.091	0.779	0.021	0.948	0.143	0.736	0.294	0.354	0.399	0.199	**-0.714**	**0.047**	0.217	0.499	0.252	0.430
Plasma Glucose[a]	**-0.707**	**0.050**	-0.509	0.110	-0.214	0.505	-0.180	0.670	*-0.523*	*0.099*	-0.224	0.484	-0.491	0.217	-0.486	0.129	-0.172	0.594
Adiponectin	-0.048	0.911	*-0.503*	*0.095*	0.147	0.649	-0.143	0.736	*0.517*	*0.085*	0.000	1.000	*-0.690*	*0.058*	-0.077	0.812	0.084	0.795

Table presenting Spearman's Rho correlation coefficients and p-values (n=8 for control, n=12 for DIO and CR groups, unless otherwise stated). Significant correlation values ($p<0.05$) are bolded, trends ($p<0.1$) are shown in italics. Abbreviations: BW, body weight; CR, caloric restriction; DIO, diet-induced obesity; DRD, dopamine receptor; eWAT, epidydimal white adipose tissue; HOMA-IR, Homeostatic Model Assessment for Insulin Resistance; TH, tyrosine hydroxylase.
[a] : n=11 for DIO.

Table 2
Multilinear regression models for predicting DRD1 and TH protein levels in iWAT.

DRD1	Model 1		TH	Model 1	
Adjusted R^2	0.437		Adjusted R^2	0.389	
p-value	**<0.001**		p-value	**<0.001**	
Variable	**β**	**p-value**	**Variable**	**β**	**p-value**
Group (diet)	**-0.669**	**<0.001**	Group (diet)	-0.055	0.732
BW gain	**-0.444**	**0.008**	BW gain	**-0.530**	**0.003**
Plasma glucose	**-0.312**	**0.033**	Plasma glucose	**-0.363**	**0.019**

Protein levels of DRD1 and TH in iWAT from all rats (n=32; 8 control, 12 DIO, 12 CR). Abbreviations: BW, body weight; DRD1, dopamine receptor D1; DIO, diet-induced obesity; eWAT, epidydimal white adipose tissue; iWAT, inguinal white adipose tissue; TH, tyrosine hydroxylase.

group, TH protein levels in eWAT tended to correlate positively with BW (p=0.088), while in the DIO group, TH tended to correlate positively with glucose levels (p=0.095). Across all groups, DRD1, DRD2, and TH protein levels in eWAT were not correlated with the markers analyzed (Supplementary Table 5).

DRD1, DRD2, and TH protein levels in human subcutaneous and omental adipose tissue

DRD1 protein levels were significantly higher in OAT of individuals with obesity ($p<0.01$, Fig. 5A), while DRD2 protein levels were significantly higher in both SAT and OAT of individuals with obesity ($p<0.05$ for SAT, $p<0.01$ for OAT), compared to lean individuals (Fig. 5B). These obesity-related upregulations in DRD1 and DRD2 protein levels were most evident among females ($p<0.10$), but due to the small sample sizes, sex differences cannot be assessed. In individuals with obesity, DRD1 protein levels were significantly higher in OAT, compared to SAT ($p<0.01$), while DRD2 levels tended to be as well (p=0.052). In lean individuals, no differences in DRD1 and DRD2 levels between SAT and OAT were found (Fig. 5A and 5B). Protein levels of TH were comparable between individuals with or without obesity in SAT and OAT. In individuals with obesity, there was a tendency for higher TH levels in OAT compared to SAT (p=0.076, Fig. 5C).

In SAT, DRD1 protein levels correlated negatively with C-peptide levels ($p<0.05$, Table 4). In OAT, DRD1 protein levels correlated positively with BMI, and SAT and OAT cell size ($p<0.05$ for all). DRD2 protein levels in OAT were positively correlated with BMI, SAT and OAT cell size, HOMA-IR, glucose, insulin, and C-peptide ($p<0.05$ for all). TH protein level in OAT was positively associated with HbA1c ($p<0.05$, Table 4).

Discussion

Obesity is associated with dysregulation of dopamine and its receptors in the brain [13,15,42] and AT [26,27] in rodents and humans, but findings in the literature are limited and conflicting regarding the direction of these changes. In this study, we used a cafeteria diet, instead of the traditional high-fat diet (HFD), to study obesity in rats, in order to more accurately emulate human obesity development.[43] Our findings provide insights into how dopaminergic pathways in the rat brain are affected by interventions with high (DIO) or low (CR) energy intake. In addition, we present dopamine receptor alterations in both rat and human AT which are partly similar to the findings we observed in the brain. To the best of our knowledge, this is the first study exploring effects of obesity on dopamine metabolism and dopamine receptors simultaneously in key brain areas involved in feeding behavior and energy balance. We also show for the first time DRD1, DRD2, and TH protein levels in human OAT from individuals with or without obesity.

Table 3
Correlations of DRD1, DRD2, and TH protein levels in rat eWAT with markers of obesity, hyperglycemia and insulin resistance within the control, DIO, or restricted group.

eWAT	DRD1						DRD2						TH					
	Control		DIO		CR		Control		DIO		CR		Control		DIO		CR	
	Rho	p-value	Rho	p-value	Rho	p-value	Rho	p-value	Rho	p-value	Rho	p-value	Rho	p-value	Rho	p-value	Rho	p-value
Adiposity measures																		
BW (g)	-0.050	0.898	-0.382	0.247	-0.255	0.450	**-0.817**	**0.007**	-0.182	0.593	**0.655**	**0.029**	*0.600*	*0.088*	-0.145	0.670	0.041	0.905
BW gain (%)	-0.233	0.546	0.327	0.326	**-0.809**	**0.003**	-0.267	0.488	0.027	0.937	0.482	0.133	0.267	0.488	0.118	0.729	-0.068	0.842
eWAT (g/kg)	*0.617*	*0.077*	-0.509	0.110	-0.155	0.650	*-0.650*	*0.058*	-0.518	0.102	0.245	0.467	0.367	0.332	-0.209	0.537	0.009	0.979
Leptin	0.000	1.000	-0.027	0.937	-0.455	0.160	**-0.750**	**0.020**	-0.036	0.915	**0.745**	**0.008**	0.100	0.798	-0.045	0.894	0.200	0.555
Hyperglycemia and insulin resistance																		
HOMA-IR[a]	0.133	0.732	0.236	0.511	-0.055	0.873	*-0.617*	*0.077*	0.297	0.405	0.409	0.212	0.367	0.332	0.333	0.347	0.141	0.679
Plasmainsulin	0.433	0.244	0.218	0.519	-0.136	0.689	*-0.583*	*0.099*	0.236	0.484	*0.591*	*0.056*	0.467	0.205	0.064	0.853	0.091	0.790
Plasma Glucose[a]	-0.209	0.589	-0.024	0.947	-0.068	0.842	0.000	1.000	0.257	0.474	-0.437	0.179	0.067	0.864	*0.557*	*0.095*	0.037	0.915
Adiponectin	**0.883**	**0.002**	-0.073	0.832	-0.018	0.958	-0.233	0.546	-0.182	0.593	-0.182	0.593	-0.133	0.732	0.018	0.958	0.000	1.000

Table presenting Spearmanś Rho correlation coefficients and p-values (n=9 for control, n=11 for DIO and CR groups, unless otherwise stated). Significant correlation values ($p<0.05$) are bolded, trends ($p<0.1$) are shown in italics. Abbreviations: BW, body weight; CR, caloric restriction; DIO, diet-induced obesity; DRD, dopamine receptor; eWAT, epidydimal white adipose tissue; HOMA-IR, Homeostatic Model Assessment for Insulin Resistance; TH, tyrosine hydroxylase.

[a] : n=10 for DIO.

Dopamine abundance in the brain

Increased dopamine levels in the Cg and NAc, being key regions in the mesocorticolimbic dopamine pathway, and the CPu, which is part of the nigrostriatal dopamine pathway, are known to be involved in reward reinforcement and preference for highly palatable foods, as well as food-seeking behavior.[30,31] Here, we demonstrated brain region-specific changes in dopamine abundance in response to a high-energy diet, with no differences in the Cg, NAc shell and Hth, but a tendency for higher dopamine levels in the NAc core and CPu of DIO rats. Since DOPAL and 3MT levels are unchanged in the CPu and NAc core of DIO rats, it seems that the enzyme activity of MAO and COMT, respectively, do not scale up in response to elevated dopamine levels. However, HVA levels and the HVA/dopamine ratio, used as a proxy for overall dopamine metabolism,[38] were increased in DIO rats, which may indicate an increased overall dopamine turnover, along with elevated dopamine levels. Although these increased dopamine levels in the CPu and NAc did not reach statistical significance after adjusting for multiple comparisons, the observed pattern aligns with a study showing increased extracellular dopamine levels in the striatum, which includes the CPu and NAc, of obesity-prone rats on HFD, when compared to obesity-resistant rats.[44] On the other hand, others have reported decreased levels of dopamine and dopaminergic-related gene expression in the NAc core of mice on HFD,[45] reduced basal dopamine levels in obesity-prone rats, even after HFD withdrawal,[46] or no change of dopamine in the NAc of rats on a cafeteria diet, compared to control rats.[47] One study with a similar experimental set-up showed decreased dopamine levels in the prefrontal cortex of DIO rats compared to control rats, but no change in CR rats.[42] Together, these studies highlight that the field is not conclusive yet regarding the direction of changes in dopamine levels induced by DIO. These discrepant findings might arise from differences in species, brain areas analyzed, techniques used to measure dopamine levels, or diet composition, as the cafeteria diet in our study included high fat, but also high sugar contents. Important to note is that MALDI-MSI provides spatial information about the distribution of dopamine but does not allow for differentiation between intra- and extracellular dopamine levels. Therefore, further research is required to elucidate intra- and extracellular changes in dopamine levels following DIO or CR.

CR increased the turnover of dopamine to DOPAL in all brain areas analyzed in this study. Since dopamine levels were unchanged in CR rats, this might point to changes in the activity of MAO. Indeed, MAO is responsive to changes in metabolic conditions, and CR has been postulated to increase its activity.[48] However, we used metabolite levels and turnover rates as a proxy for enzymatic activity, so to be able to draw definite conclusions regarding changes in enzymatic activity, direct enzymatic measures are necessary.

In the present study, dopamine levels in the NAc core were associated with markers of hyperglycemia and whole-body insulin resistance, and HOMA-IR was the strongest predictor of dopamine levels in the NAc. Insulin signaling in the brain has been associated with whole-body insulin sensitivity,[49] and the NAc core has been reported as a primary target of HFD-induced insulin resistance which can drive changes in reward sensitivity and promote food overconsumption.[16] Our findings support a role for the NAc core in metabolic dysregulation, potentially mediated by neuronal insulin resistance.

Dopamine receptor levels in the brain

We found increased DRD1 expression in the Cg and the CPu, and increased DRD2 expression in the CPu and NAc core, VMH and LH, following DIO. Dopaminergic signaling in the Cg is associated with effort-based decision making through DRD1, but not DRD2,[50] and activation of DRD1 in the prefrontal cortex increases food intake in sated animals.[51] Therefore, upregulation of DRD1 in DIO rats might lead to a stronger drive for food-seeking, driven by an amplified hedonic drive for

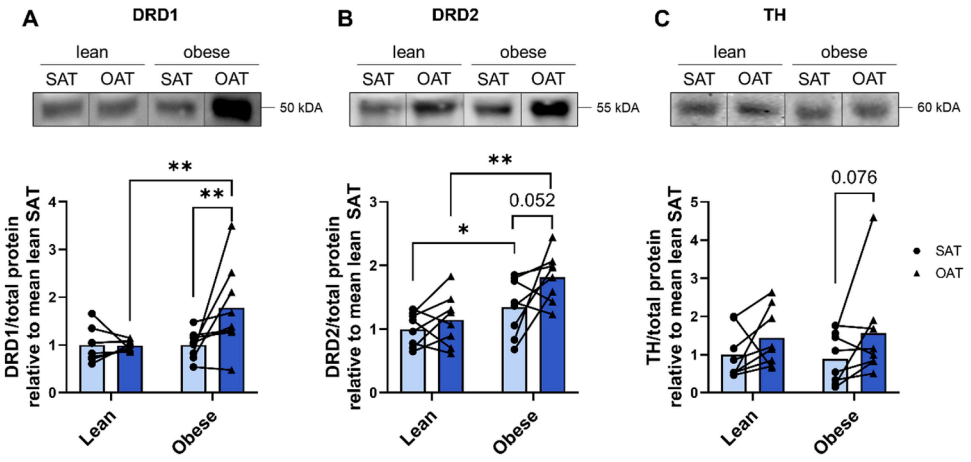

Fig. 5. Dopamine receptors and TH protein levels in paired human SAT and OAT from individuals with and without obesity. Representative immunoblot and protein quantification of DRD1 (A), DRD2 (B), and TH protein (C) levels in SAT and OAT from subjects with or without obesity (n=8/group). Bands are derived from different parts of the same gel. Protein levels were normalized to total protein (Supplementary Figure 2) and to a reference sample loaded on each gel. Values are relative to the mean of the lean SAT group. Data are shown as mean ± SEM. * $p<0.05$, ** $p<0.01$. Abbreviations: OAT, omental adipose tissue; SAT, subcutaneous adipose tissue.

Table 4
Correlations of human DRD1, DRD2, and TH protein levels with markers of adiposity, hyperglycemia and insulin resistance in subcutaneous adipose tissue (SAT) and omental adipose tissue (OAT).

	SAT						OAT					
	DRD1		DRD2		TH		DRD1		DRD2		TH	
Variable	Rho	p-value	Rho	p-value	Rho	p-value	Rho	p-value	Rho	p-value	Rho	p-value
Adiposity measures												
BMI	0.288	0.279	*0.482*	*0.058*	-0.244	0.362	**0.629**	**0.009**	**0.665**	**0.005**	-0.021	0.940
WHR	-0.384	0.142	-0.219	0.415	0.096	0.725	0.004	0.987	-0.038	0.888	-0.094	0.729
SAT cell size (μm)[a]	-0.112	0.703	0.310	0.281	-0.327	0.253	**0.798**	**<.001**	**0.604**	**0.022**	-0.147	0.615
OAT cell size (μm)[b]	-0.066	0.831	0.467	0.108	-0.176	0.566	**0.665**	**0.013**	**0.665**	**0.013**	-0.011	0.972
Hyperglycaemia and insulin resistance												
HbA1c	-0.227	0.399	0.147	0.588	0.363	0.167	0.173	0.521	*0.446*	*0.084*	**0.508**	**0.045**
HOMA-IR[c]	-0.246	0.376	0.118	0.676	-0.100	0.723	0.429	0.111	**0.625**	**0.013**	-0.004	0.990
Fasting glucose	-0.204	0.449	0.247	0.357	0.306	0.249	0.344	0.193	**0.568**	**0.022**	0.036	0.896
Fasting insulin[c]	-0.286	0.302	0.111	0.694	-0.079	0.781	0.425	0.114	**0.639**	**0.010**	0.032	0.909
C-peptide[b]	**-0.619**	**0.024**	-0.052	0.865	-0.113	0.714	0.338	0.258	**0.553**	**0.050**	-0.063	0.837

Table presents Spearman's Rho correlation coefficient and p-values (n=16, unless otherwise stated). Significant correlation values ($p<0.05$) are bolded, trends ($p<0.1$) shown in italics. Abbreviations: BMI, body mass index; HbA1c, glycated hemoglobin; HOMA-IR, Homeostatic Model Assessment for Insulin Resistance; OAT, omental adipose tissue; SAT, subcutaneous adipose tissue; WHR, waist-hip ratio

[a] n=14
[b] n=13
[c] n=15

palatable foods. The DIO rats in this project did not show an altered behavioral profile (e.g., risk assessment or risk seeking) in the Multivariate Concentric Square Field (MCSF).[29] An interesting follow-up experiment could be to evaluate how the presence of a motivational stimulus (e.g., palatable food) in the MCSF influences effort-based decision making, and whether this is mediated by DRD1 in the Cg. We furthermore show that the DRD1 and DRD2 abundance is increased in the CPu following energy excess, suggesting that both receptors are responsive to changes in energy balance. In the CPu, DRD1-expressing neurons facilitate, while DRD2-expression neurons inhibit, movement and reward-driven behavior, and the balance between these receptors is of paramount importance.[52] Upregulation of both receptors might imply an overall heightened responsiveness to dopamine. However, DRD1 and DRD2 are responsive to different levels of dopamine,[53] meaning that a shift in their ratio might change the downstream effects. Therefore, calculating the DRD1-to-DRD2 ratio might reveal a potential imbalance between these receptors. Unfortunately, this ratio could not be measured in this study.

To continue, we showed a tendency for increased DRD2 levels in the NAc core following both energy excess and energy restriction. In line with our data, DIO has been associated with elevated DRD2 protein levels in the CPu and NAc of mice.[54] In contrast, downregulated *DRD1* and *DRD2* levels were seen in the NAc of HFD mice, as well as lower dopamine levels.[45] These discrepant findings might be explained by differences in diet but there can also be a discrepancy between the protein and mRNA levels for DRD1 and DRD2.[26] In humans, previous work has reported reduced, unchanged, or increased striatal DRD2 receptor binding in obesity.[13,55,56] However, most knowledge on altered dopamine signaling has come from imaging techniques using radiolabeled tracers.[12] These techniques pose challenges to interpret dopamine binding potential, as it may reflect receptor density or affinity, or competition with endogenous dopamine for receptor binding.[12]

An interesting observation was the U-shaped relationship between DRD2 in the Cg, CPu, and NAc core with BW, and between DRD1 in the CPu and BW. With these regions being involved in the reward system, these findings align with a non-linear relationship that has been reported between BMI and sensitivity to reward [57] and indicate an interesting connection between dopamine receptors in the brain and obesity

that deserves more attention.

Surprisingly, we found similar changes in the abundance of DRD1 and DRD2 in the Cg, CPu, and NAc core following CR as after DIO. Importantly, even though both dietary interventions induce similar changes in DRD1 and DRD2 abundance, the downstream effect might still differ due to differences in dopamine availability. Only DIO rats exhibited elevated dopamine levels as well, and receptor affinity to dopamine levels is not the same for DRD1 and DRD2.[53]

Regarding hypothalamic areas, DIO increased the abundance of DRD2 in the VMH, well recognized as the satiety center,[58] and tended to increase DRD2 in the LH, relevant for regulating both homeostatic energy intake and reward-related behavior.[59] Activation of DRD2 in the VMH modulated plasma leptin and glucose levels.[60] In the LH, dopamine is postulated to activate orexin neurons via DRD2.[61] Therefore, future experiments could test whether elevation of DRD2 in the LH increases the activity of orexinergic neurons and if this stimulates feeding behavior. Furthermore, DRD2 activation in the LH reduced BW gain and fat mass in rodents,[19] indicating that upregulation of DRD2 could also be a counterregulatory response aiming to limit further weight gain or fat accumulation.

Taken together, dopamine receptors in the Cg, CPu, and NAc Core responded to both energy excess and energy restriction and revealed a non-linear relationship with markers of adiposity, reinforcing the intricate role of the reward system in metabolic (dys)regulation. Hypothalamic areas responded specifically to energy excess by increasing DRD2 protein levels, that could either aggravate or counteract the perturbation. Further research is warranted to characterize causal mechanisms.

Overall, increased dopamine and dopamine receptor abundance in DIO rats in crucial reward regions of the brain might indicate a heightened sensitivity to reward in the form of highly palatable food,[62] rather than a reward deficiency that has been proposed as a mechanism for overeating and contributing to the development of obesity.[13] But perhaps, as postulated before, a reward deficiency emerges only after obesity has reached a more severe stage or has persisted over a longer period.[63]

Dopamine receptors in adipose tissue

We show that both dietary interventions led to a downregulation of DRD1 in iWAT and eWAT. Limited data exists on the role of dopamine receptors in AT, and the effects of obesity or T2D on receptor levels. Downregulation of *DRD1* mRNA levels in iWAT has been reported in DIO mice,[64] while no effect of high-calorie diet was found on DRD1 protein levels in eWAT of Goto Kakizaki (GK) rats.[27] This discrepancy could be explained by different diets or animal models, as the GK rat model is a genetic model of T2D with pancreatic β cell failure.[65] Activation of DRD1 in mature 3T3-L1 adipocytes stimulated lipolysis,[66] which could imply that downregulation of DRD1 reduces lipolysis. At the same time, both diets increased DRD2 protein levels in this study, but only in iWAT, suggesting a fat-depot specific effect on this receptor. Previous work has shown that DRD2 activation inhibits isoproterenol-stimulated lipolysis in human AT *ex vivo*.[26] Taken together, downregulation of DRD1 and upregulation of DRD2 in iWAT from both DIO and CR rats might reflect anti-lipolytic effects to regulate fat mobilization. In DIO rats, this could promote subcutaneous AT lipid storage and prevent dyslipidemia, as observed in rats treated with bromocriptine,[27] whereas in CR rats, it might again be a defense mechanism to conserve energy reserves. In DIO rats, decreased TH protein levels in iWAT could reflect reduced sympathetic nerve density and local dopamine and noradrenaline release. Thus, a decrease in sympathetic nerve density, together with increased DRD2 and reduced DRD1 protein levels, could promote lipid storage in iWAT.

Regarding human AT, we show an upregulation of DRD2 protein levels in SAT, as well as in OAT, in individuals with obesity. DRD2 upregulation in SAT is in line with the DIO rat findings, and also with previously published human data from our group.[26] In contrast, DRD1 protein levels were unchanged in SAT and upregulated in OAT from individuals with obesity, thus markedly different from the downregulation found in both depots of DIO rats. Furthermore, these results suggest a depot-specific effect on DRD1. Interestingly, in paired AT samples from individuals with obesity, we observed higher DRD1 and DRD2 protein levels in OAT, compared to SAT, which was not seen in lean individuals. This suggests an enhanced capacity of OAT to respond to dopaminergic signals in human obesity. Moreover, in OAT, both receptors showed a strong positive correlation with BMI, whereas only DRD2 was associated with markers of hyperglycemia and insulin resistance. One study showed a trend to reduced *DRD1* gene expression in visceral AT from insulin-resistant individuals with obesity and T2D, compared to insulin-sensitive individuals with obesity, while *DRD2* levels were not affected by insulin resistance.[27] Thus, obesity and insulin resistance may have separate connections to *DRD1* expression, but there can also be a discrepancy between the protein and mRNA levels for DRD1 and DRD2, as we have previously published.[26]

Taken together, obesity has partly discordant effects on dopamine receptors in rat and human AT, suggesting species-specific differences in AT metabolism and regulation. However, an intriguing finding was the upregulation of DRD2 by DIO in both energy-regulating areas of the brain and iWAT of rats, as well as in both SAT and OAT of humans with obesity. The seemingly concerted regulation warrants further exploration, e.g., on the role of sympathetic nerves connecting the brain and periphery. It also highlights the relevance of DRD2 in regulating or responding to metabolic changes.

Limitations

This study has some limitations. MALDI-MSI provides spatial information about the distribution of dopamine but does not differentiate the source. Therefore, we cannot conclude whether changes in dopamine abundance are due to altered local dopamine synthesis at the terminal level, or alterations in dopaminergic signaling from e.g., the ventral tegmental area. Another technical limitation is the sample size for the brain analyses, which might have limited our ability to detect statistically significant differences after adjusting for multiple comparisons. While we observe several trends pointing to effects of metabolic status on dopamine signaling, future studies in larger cohorts are required to confirm these findings. Furthermore, we also lack direct measurements of post-synaptic dopamine receptor signaling in the brain or on dopamine metabolism in peripheral tissue, including AT. To continue, not all rats were euthanized and sampled under standardized conditions, e.g., fasting and at a specific time of the day.[29] This may influence results of metabolic parameters and of dopamine levels, which are increased upon ingestion of palatable foods,[67] and should be considered when interpreting these results. Lastly, only male rats were investigated here. Given the high prevalence of overweight and obesity in women,[68] and the underrepresentation of females in animal and human studies,[69] future studies should be conducted on both sexes.

In summary, caloric excess, in the form of highly palatable foods, and caloric restriction affect elevated DRD1 and DRD2 receptor levels in the rat brain in a region-specific manner. The Cg, CPu and NAc core were affected by both caloric excess and restriction, while hypothalamic areas responded specifically to caloric excess. In rat AT, both dietary interventions similarly altered DRD1 and DRD2 receptor abundance, while sympathetic nerve density was only reduced by DIO in a fat-depot specific manner. Lastly, in human AT, obesity elevated both DRD1 and DRD2 in OAT, while only DRD2 was upregulated in SAT as well, highlighting the fat-depot specific effects of obesity, which requires further examination.

The partly divergent alterations of dopamine receptor abundances in rat and human AT depots in obesity suggest species- and depot-specific differences. This also holds true for the role of the dopaminergic brain network. Obesity in humans is inherently more complex than in rodent models in terms of numerous genetic, environmental, and psychological

factors.[70] Many of these are not well reflected in a DIO rat model and further human studies are needed. Nonetheless, the current findings in the rat brain are important to guide the design of clinical neuroimaging studies using PET, e.g. with radioligands for dopamine receptors, as well as functional MRI targeting regions of interest. Such work will enhance understanding of the brain's role in development and reversal of human obesity and T2D.

Conclusions

Overall, we demonstrate that excess energy intake in male rats leads to elevated levels of dopamine or some of its metabolites, and upregulation of DRD1 or DRD2 in the cingulate cortex, caudate putamen and nucleus accumbens. This may contribute to adaptations in motivated behavior, reward processing, and overall energy balance regulation. A similar direction of changes in dopamine receptor abundance following caloric restriction was surprising. However, this may be a reward response during caloric excess that further aggravates overeating, while during caloric deficit it may serve as a defense mechanism to increase energy stores. Dopaminergic alterations may also be relevant for the development of insulin resistance and dysglycemia. In human obesity, DRD1 was upregulated in OAT, whereas DRD2 was upregulated in both SAT and OAT, which was partly different from rat AT. There may thus be an increased capacity in human OAT to respond to dopaminergic signals. These results highlight the complex perturbations of obesity found in dopaminergic pathways in both the brain and periphery. The mechanistic and functional details and the role in organ crosstalk requires further research including experimental pharmacological interventions. Further studies are also warranted to elucidate alterations in dopaminergic pathways in the brain and AT during the development of T2D. Such work may enable the discovery of novel principles for prevention and treatment of metabolic disorders.

Funding

Swedish Diabetes Foundation (DIA2021-661; DIA2021-618); Swedish National Strategic Research Initiative EXODIAB; Swedish Research Council (2024-03344); Swedish Foundation for Strategic Research (CMP22-0014); the Family Ernfors Foundation; P.O Zetterling Foundation; NovoNordisk Foundation (NNF20OC0063864; NNF23OC0084483); Agnes and Mac Rudberg Foundation; Uppsala Diabetes Centre; European Commission Horizon RIA project PAS GRAS 101080329; and Uppsala University Hospital ALF grants.

Data availability

Datasets generated and/or analyzed during the current study are available from the corresponding author on reasonable request.

CRediT authorship contribution statement

Fleur W Hukema: Writing – review & editing, Writing – original draft, Project administration, Investigation, Formal analysis, Conceptualization. **Susanne Hetty:** Writing – review & editing, Supervision, Project administration, Investigation, Formal analysis, Conceptualization. **Christakis Kagios:** Writing – review & editing, Investigation, Conceptualization. **Sofia Zelleroth:** Writing – review & editing, Investigation, Formal analysis, Conceptualization. **Giovanni Fanni:** Writing – review & editing, Investigation, Conceptualization. **Maria J Pereira:** Writing – review & editing, Supervision, Resources, Project administration, Funding acquisition, Conceptualization. **Maria K Svensson:** Writing – review & editing, Resources. **Magnus Sundbom:** Writing – review & editing, Resources. **Anna Nilsson:** Writing – review & editing, Investigation, Conceptualization. **Per E Andrén:** Writing – review & editing, Resources, Funding acquisition, Conceptualization. **Erika Roman:** Writing – review & editing, Resources, Funding acquisition, Conceptualization. **Jan W Eriksson:** Writing – review & editing, Supervision, Resources, Project administration, Funding acquisition, Conceptualization.

Acknowledgements

We want to thank Stina Lundberg for technical assistance with the animal work. We are grateful to our colleagues at Clinical Diabetes and Metabolism, Dept. of Medical Sciences, Uppsala University and at Uppsala University Hospital for making this study possible. Lastly, we thank all participants in the study. The authors confirm they have read the journal's policy on disclosure of potential conflicts of interest and have nothing to disclose. All authors also confirm they have read the journal's authorship agreement and that the manuscript has been reviewed by and approved by all named authors.

Supplementary materials

Supplementary material associated with this article can be found, in the online version, at doi:10.1016/j.trsl.2025.05.001.

References

1. World Obesity Federation. *Prevalence of obesity*; 2024. Accessed December 18, 2024 https://www.worldobesity.org/about/about-obesity/prevalence-of-obesity.
2. Fahed G, Aoun L, Bou Zerdan M, et al. Metabolic Syndrome: updates on pathophysiology and management in 2021. *Int J Mol Sci*. 2022;23(2):786. https://doi.org/10.3390/ijms23020786.
3. Fanni G. Diabetes is not (only) a disorder of glucose metabolism!. *Diabet Med*. 2021;38(2):9–10. https://doi.org/10.1111/dme.14464.
4. Riaz H, Khan MS, Siddiqi TJ, et al. Association between obesity and cardiovascular outcomes: A systematic review and meta-analysis of mendelian randomization studies. *JAMA Netw Open*. 2018;1(7), e183788. https://doi.org/10.1001/JAMANETWORKOPEN.2018.3788. -e183788.
5. Lundqvist MH, Pereira MJ, Wiklund U, Hetty S, Eriksson JW. Autonomic nervous system responses to hypo- and hyperglycemia in type 2 diabetes and prediabetes. *Eur J Endocrinol*. 2024;191(5):499–508. https://doi.org/10.1093/ejendo/lvae130.
6. Saeed S, Bonnefond A, Froguel P. Obesity: exploring its connection to brain function through genetic and genomic perspectives. *Mol Psychiatry*. 2024. https://doi.org/10.1038/s41380-024-02737-9. Published online September 5,.
7. Fanni G, Kvernby S, Radhi S, et al. Regional brain glucose uptake following gastric bypass surgery during normo- and hypoglycemic clamp: a pilot FDG-PET study. *Endocrine*. 2024. https://doi.org/10.1007/s12020-024-04127-1. Published online December 7.
8. Almby KE, Lundqvist MH, Abrahamsson N, et al. Effects of gastric bypass surgery on the brain: simultaneous assessment of glucose uptake, blood flow, neural activity, and cognitive function during normo- and hypoglycemia. *Diabetes*. 2021;70(6):1265–1277. https://doi.org/10.2337/db20-1172.
9. Klein MO, Battagello DS, Cardoso AR, Hauser DN, Bittencourt JC, Correa RG. Dopamine: functions, signaling, and association with neurological diseases. *Cell Mol Neurobiol*. 2019;39(1):31–59. https://doi.org/10.1007/s10571-018-0632-3.
10. Gurevich EV, Gainetdinov RR, Gurevich VV. G protein-coupled receptor kinases as regulators of dopamine receptor functions. *Pharmacol Res*. 2016;111:1–16. https://doi.org/10.1016/j.phrs.2016.05.010.
11. Horstmann A. It wasn't me; it was my brain – Obesity-associated characteristics of brain circuits governing decision-making. *Physiol Behav*. 2017;176:125–133. https://doi.org/10.1016/j.physbeh.2017.04.001.
12. Janssen LK, Horstmann A. Molecular imaging of Central dopamine in obesity: A qualitative review across substrates and radiotracers. *Brain Sci*. 2022;12(4):486. https://doi.org/10.3390/brainsci12040486.
13. Wang GJ, Volkow ND, Logan J, et al. Brain dopamine and obesity. *The Lancet*. 2001;357(9253):354–357. https://doi.org/10.1016/S0140-6736(00)03643-6.
14. Ribeiro G, Maia A, Cotovio G, Oliveira FPM, Costa DC, Oliveira-Maia AJ. Striatal dopamine D2-like receptors availability in obesity and its modulation by bariatric surgery: a systematic review and meta-analysis. *Sci Rep*. 2023;13(1):1–12. https://doi.org/10.1038/s41598-023-31250-2, *2023 13:1*.
15. Guo J, Simmons WK, Herscovitch P, Martin A, Hall KD. Striatal dopamine D2-like receptor correlation patterns with human obesity and opportunistic eating behavior. *Mol Psychiatry*. 2014;19(10):1078–1084. https://doi.org/10.1038/mp.2014.102.
16. Wallace CW, Fordahl SC. Obesity and dietary fat influence dopamine neurotransmission: exploring the convergence of metabolic state, physiological stress, and inflammation on dopaminergic control of food intake. *Nutr Res Rev*. 2022;35(2):236–251. https://doi.org/10.1017/S0954422421000196.
17. Bromocriptine DeFronzoRA. A sympatholytic, D2-dopamine agonist for the treatment of type 2 diabetes. *Diabetes Care*. 2011;34(4):789–794. https://doi.org/10.2337/DC11-0064.
18. Birhan MT, Ayele TM, Abebe FW, Dgnew FN. Effect of bromocriptine on glycemic control, risk of cardiovascular diseases and weight in patients with type 2 diabetes: a

systematic review. *Diabetol Metab Syndr*. 2023;15(1):1–7. https://doi.org/10.1186/S13098-023-01073-2/TABLES/2.
19. Folgueira C, Beiroa D, Porteiro B, et al. Hypothalamic dopamine signalling regulates brown fat thermogenesis. *Nat Metab*. 2019;1(8):811–829. https://doi.org/10.1038/s42255-019-0099-7.
20. Bartness TJ, Liu Y, Shrestha YB, Ryu V. Neural innervation of white adipose tissue and the control of lipolysis. *Front Neuroendocrinol*. 2014;35(4):473–493. https://doi.org/10.1016/j.yfrne.2014.04.001.
21. Daubner SC, Le T, Wang S. Tyrosine hydroxylase and regulation of dopamine synthesis. *Arch Biochem Biophys*. 2011;508(1):1–12. https://doi.org/10.1016/j.abb.2010.12.017.
22. Willows JW, Gunsch G, Paradie E, et al. Schwann cells contribute to demyelinating diabetic neuropathy and nerve terminal structures in white adipose tissue. *iScience*. 2023;26(3), 106189. https://doi.org/10.1016/j.isci.2023.106189.
23. Chi J, Wu Z, Choi CHJ, et al. Three-dimensional adipose tissue imaging reveals regional variation in beige fat biogenesis and PRDM16-dependent sympathetic neurite density. *Cell Metab*. 2018;27(1):226–236.e3. https://doi.org/10.1016/j.cmet.2017.12.011.
24. Perdikari A, Cacciottolo T, Henning E, Mendes de Oliveira E, Keogh JM, Farooqi IS. Visualization of sympathetic neural innervation in human white adipose tissue. *Open Biol*. 2022;12(3). https://doi.org/10.1098/rsob.210345.
25. Goldstein DS, Holmes C. Neuronal source of plasma dopamine. *Clin Chem*. 2008;54(11):1864–1871. https://doi.org/10.1373/clinchem.2008.107193.
26. Vranic M, Ahmed F, Kristófi R, et al. Subcutaneous adipose tissue dopamine D2 receptor is increased in prediabetes and T2D. *Endocrine*. 2023;83(2):378–391. https://doi.org/10.1007/s12020-023-03525-1.
27. Tavares G, Marques D, Barra C, et al. Dopamine D2 receptor agonist, bromocriptine, remodels adipose tissue dopaminergic signalling and upregulates catabolic pathways, improving metabolic profile in type 2 diabetes. *Mol Metab*. 2021;51, 101241. https://doi.org/10.1016/j.molmet.2021.101241.
28. Zhu Y, Yao L, Gallo-Ferraz AL, et al. Sympathetic neuropeptide Y protects from obesity by sustaining thermogenic fat. *Nature*. 2024;634(8032):243–250. https://doi.org/10.1038/s41586-024-07863-6.
29. Kagios C, Hetty S, Grönbladh A, Pereira MJ, Eriksson JW, Roman E. Cafeteria diet and caloric restriction affect metabolic but not behavioral characteristics in male Wistar rats. *Physiol Behav*. 2025;288, 114731. https://doi.org/10.1016/j.physbeh.2024.114731.
30. Benton D, Young HA. A meta-analysis of the relationship between brain dopamine receptors and obesity: a matter of changes in behavior rather than food addiction? *Int J Obes*. 2016;40(S1):S12–S21. https://doi.org/10.1038/ijo.2016.9.
31. Wise RA. Roles for nigrostriatal–not just mesocorticolimbic–dopamine in reward and addiction. *Trends Neurosci*. 2009;32(10):517–524. https://doi.org/10.1016/j.tins.2009.06.004.
32. Qi-Lytle X, Sayers S, Wagner EJ. Current review of the function and regulation of tuberoinfundibular dopamine neurons. *Int J Mol Sci*. 2023;25(1). https://doi.org/10.3390/ijms25010110.
33. Zhang X, van den Pol AN. Hypothalamic arcuate nucleus tyrosine hydroxylase neurons play orexigenic role in energy homeostasis. *Nat Neurosci*. 2016;19(10):1341–1347. https://doi.org/10.1038/nn.4372.
34. Percie du Sert N, Hurst V, Ahluwalia A, et al. The ARRIVE guidelines 2.0: updated guidelines for reporting animal research. *PLoS Biol*. 2020;18(7), e3000410. https://doi.org/10.1371/journal.pbio.3000410.
35. Pereira MJ, Mathioudaki A, Otero AG, et al. Renal sinus adipose tissue: exploratory study of metabolic features and transcriptome compared with omental and subcutaneous adipose tissue. *Obesity*. 2024;32(10):1870–1884. https://doi.org/10.1002/oby.24114.
36. Paxinos G, Watson C. *The rat brain in stereotaxic coordinates atlas*. 7th ed. Academic Press; 2014.
37. Zhang S, Wang R, Wang G. Impact of dopamine oxidation on dopaminergic neurodegeneration. *ACS Chem Neurosci*. 2019;10(2):945–953. https://doi.org/10.1021/acschemneuro.8b00454.
38. Amin F, Davidson M, Davis KL. Homovanillic acid measurement in clinical research: a review of methodology. *Schizophr Bull*. 1992;18(1):123–148. https://doi.org/10.1093/schbul/18.1.123.
39. Shariatgorji R, Nilsson A, Fridjonsdottir E, et al. Spatial visualization of comprehensive brain neurotransmitter systems and neuroactive substances by selective in situ chemical derivatization mass spectrometry imaging. *Nat Protoc*. 2021;16(7):3298–3321. https://doi.org/10.1038/s41596-021-00538-w.
40. Shariatgorji M, Nilsson A, Fridjonsdottir E, et al. Comprehensive mapping of neurotransmitter networks by MALDI–MS imaging. *Nat Methods*. 2019;16(10):1021–1028. https://doi.org/10.1038/s41592-019-0551-3.
41. Martire SI, Holmes N, Westbrook RF, Morris MJ. Altered feeding patterns in rats exposed to a palatable cafeteria diet: increased snacking and its implications for development of obesity. *PLoS One*. 2013;8(4), e60407. https://doi.org/10.1371/journal.pone.0060407.
42. Jantsch J, Rodrigues F da S, Fraga G, de F, et al. Calorie restriction mitigates metabolic, behavioral and neurochemical effects of cafeteria diet in aged male rats. *J Nutr Biochem*. 2023;119, 109371. https://doi.org/10.1016/j.jnutbio.2023.109371.
43. Sampey BP, Vanhoose AM, Winfield HM, et al. Cafeteria diet is a robust model of Human metabolic syndrome with liver and adipose inflammation: comparison to high-fat diet. *Obesity*. 2011;19(6):1109–1117. https://doi.org/10.1038/oby.2011.18.
44. Narayanaswami V, Thompson AC, Cassis LA, Bardo MT, Dwoskin LP. Diet-induced obesity: dopamine transporter function, impulsivity and motivation. *Int J Obes*. 2013;37(8):1095–1103. https://doi.org/10.1038/ijo.2012.178.
45. Carlin J, Hill-Smith TE, Lucki I, Reyes TM. Reversal of dopamine system dysfunction in response to high-fat diet. *Obesity*. 2013;21(12):2513–2521. https://doi.org/10.1002/oby.20374.
46. Rada P, Bocarsly ME, Barson JR, Hoebel BG, Leibowitz SF. Reduced accumbens dopamine in Sprague–Dawley rats prone to overeating a fat-rich diet. *Physiol Behav*. 2010;101(3):394–400. https://doi.org/10.1016/j.physbeh.2010.07.005.
47. Vindas-Smith R, Quesada D, Hernández-Solano MI, et al. Fat intake and obesity-related parameters predict striatal BDNF gene expression and dopamine metabolite levels in cafeteria diet-fed rats. *Neuroscience*. 2022;491:225–239. https://doi.org/10.1016/j.neuroscience.2022.03.042.
48. Drew LJ, Hen R. Food for thought: linking caloric intake to behavior via sirtuin activity. *Cell*. 2011;147(7):1436–1437. https://doi.org/10.1016/j.cell.2011.11.052.
49. Heni M, Wagner R, Kullmann S, et al. Central Insulin Administration improves whole-body Insulin sensitivity via hypothalamus and parasympathetic outputs in men. *Diabetes*. 2014;63(12):4083–4088. https://doi.org/10.2337/db14-0477.
50. Schweimer J, Hauber W. Dopamine D1 receptors in the anterior cingulate cortex regulate effort-based decision making. *Learn Mem*. 2006;13(6):777–782. https://doi.org/10.1101/lm.409306.
51. Land BB, Narayanan NS, Liu RJ, et al. Medial prefrontal D1 dopamine neurons control food intake. *Nat Neurosci*. 2014;17(2):248–253. https://doi.org/10.1038/nn.3625.
52. Young C, Reddy V, Sonne J. *Neuroanatomy, basal ganglia*. 2023.
53. Marcellino D, Kehr J, Agnati LF, Fuxe K. Increased affinity of dopamine for D_2 -like versus D_1 -like receptors. Relevance for volume transmission in interpreting PET findings. *Synapse*. 2012;66(3):196–203. https://doi.org/10.1002/syn.21501.
54. South T, Huang XF. High-fat diet exposure increases dopamine D2 receptor and decreases dopamine transporter receptor binding density in the nucleus accumbens and caudate putamen of mice. *Neurochem Res*. 2008;33(3):598–605. https://doi.org/10.1007/s11064-007-9483-x.
55. Gaiser EC, Gallezot JD, Worhunsky PD, et al. Elevated dopamine D2/3 receptor availability in obese individuals: A PET imaging study with [11C](+)PHNO. *Neuropsychopharmacology*. 2016;41(13):3042–3050. https://doi.org/10.1038/npp.2016.115.
56. van de Giessen E, Celik F, Schweitzer DH, van den Brink W, Booij J. Dopamine $D_{2/3}$ receptor availability and amphetamine-induced dopamine release in obesity. *J Psychopharmacol*. 2014;28(9):866–873. https://doi.org/10.1177/0269881114531664.
57. Davis C, Fox J. Sensitivity to reward and body mass index (BMI): evidence for a non-linear relationship. *Appetite*. 2008;50(1):43–49. https://doi.org/10.1016/j.appet.2007.05.007.
58. Zhang J, Chen D, Sweeney P, Yang Y. An excitatory ventromedial hypothalamus to paraventricular thalamus circuit that suppresses food intake. *Nat Commun*. 2020;11(1):6326. https://doi.org/10.1038/s41467-020-20093-4.
59. Goel M, Mittal A, Jain VR, et al. Integrative functions of the hypothalamus: linking cognition, emotion and physiology for well-being and adaptability. *Ann Neurosci*. 2024. https://doi.org/10.1177/09727531241255492. Published online June 12,.
60. Ghasemi M, Mehranfard N, Alaei H. Modulatory effect of ventromedial hypothalamic D2 receptors on leptin and glucose concentration. *Physiology and Pharmacology*. 2018;22(2):124–132. Accessed March 14, 2025 https://ppj.phypha.ir/article-1-1364-en.html.
61. Harada M, Capdevila LS, Wilhelm M, Burdakov D, Patriarchi T. Stimulation of VTA dopamine inputs to LH upregulates orexin neuronal activity in a DRD2-dependent manner. *Elife*. 2024;12. https://doi.org/10.7554/eLife.90158.3.
62. Franken IHA, Muris P. Individual differences in reward sensitivity are related to food craving and relative body weight in healthy women. *Appetite*. 2005;45(2):198–201. https://doi.org/10.1016/j.appet.2005.04.004.
63. Horstmann A, Fenske WK, Hankir MK. Argument for a non-linear relationship between severity of human obesity and dopaminergic tone. *Obesity Reviews*. 2015;16(10):821–830. https://doi.org/10.1111/obr.12303.
64. Al Mahri S, Okla M, Rashid M, et al. Profiling of G-protein coupled receptors in adipose tissue and differentiating adipocytes offers a translational resource for obesity/metabolic research. *Cells*. 2023;12(3):377. https://doi.org/10.3390/cells12030377.
65. Guest PC. Characterization of the Goto-Kakizaki (GK) rat model of type 2 diabetes. *Methods Mol Biol*. 2019;1916:203–211. https://doi.org/10.1007/978-1-4939-8994-2_19.
66. Yu J, Zhu J, Deng J, et al. Dopamine receptor D1 signaling stimulates lipolysis and browning of white adipocytes. *Biochem Biophys Res Commun*. 2022;588:83–89. https://doi.org/10.1016/j.bbrc.2021.12.040.
67. Thanarajah SE, Backes H, DiFeliceantonio AG, et al. Food intake recruits orosensory and post-ingestive dopaminergic circuits to affect eating desire in humans. *Cell Metab*. 2019;29(3):695–706.e4. https://doi.org/10.1016/j.cmet.2018.12.006.
68. WHO I. *Obesity and overweight*; 2024. March 1,Accessed November 25, 2024 https://www.who.int/en/news-room/fact-sheets/detail/obesity-and-overweight.
69. Lalanza JF, Snoeren EMS. The cafeteria diet: A standardized protocol and its effects on behavior. *Neurosci Biobehav Rev*. 2021;122:92–119. https://doi.org/10.1016/j.neubiorev.2020.11.003.
70. Loos RJF, Yeo GSH. The genetics of obesity: From discovery to biology. *Nat Rev Genet*. 2022;23(2):120–133. https://doi.org/10.1038/s41576-021-00414-z.